

Insight into the Chemistry of Flavin Reduction and Oxidation in *Escherichia coli* Dihydroorotate Dehydrogenase Obtained by Rapid Reaction Studies[†]

Bruce A. Palfey,^{*,‡} Olof Björnberg,[§] and Kaj Frank Jensen[§]

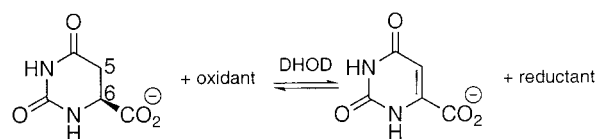
Department of Biological Chemistry, University of Michigan, Ann Arbor, Michigan 48109-0606, and Department of Biological Chemistry, Institute for Molecular Biology, University of Copenhagen, Denmark

Received November 7, 2000; Revised Manuscript Received February 5, 2001

ABSTRACT: Dihydroorotate dehydrogenase (DHOD) oxidizes dihydroorotate (DHO) to orotate in the only redox reaction of pyrimidine biosynthesis. The enzyme from *Escherichia coli* is a membrane-bound FMN-containing enzyme that is thought to use ubiquinone as the oxidizing substrate. The chemistry of the reduction of the flavin in DHOD from *E. coli* by the substrate dihydroorotate (DHO) was studied at 4 °C in anaerobic stopped-flow experiments conducted over a broad range of pH values. A Michaelis complex that was characterized by a ~20 nm red-shift of the oxidized flavin absorbance formed within the dead-time of the stopped-flow instrument (~1 ms) upon mixing with DHO. The flavin of the intermediate was reduced by DHO, forming a reduced flavin–orotate charge-transfer complex. The rate constant for the flavin reduction reaction increased with pH, from a value of 1 s⁻¹ at pH 6.5 to ~360 s⁻¹ at pH values greater than an observed pK_a of 9.5 which was ascribed to Ser175, the active-site base. At all pH values, the reduced flavin–orotate charge-transfer complex dissociated too slowly to be catalytically relevant. Therefore, the oxidizing quinone substrate must bind to the reduced enzyme–orotate complex at a site distinct from the substrate binding site, in agreement with steady-state kinetic studies [Björnberg, O., Grüner, A.-C., Roepstorff, P., and Jensen, K. F. (1999) *Biochemistry* 38, 2899–2908]. Menadione was used as a model quinone substrate to oxidize dithionite-reduced DHOD. The reduced enzyme–orotate complex reacted rapidly with menadione (180 s⁻¹), demonstrating that the reduced enzyme–orotate complex is a catalytically competent intermediate.

Dihydroorotate dehydrogenase (DHOD;¹ EC 1.3.3.1) catalyzes the oxidation of dihydroorotate (DHO) to orotate (Scheme 1), the only redox reaction in the pyrimidine biosynthetic pathway. Three groups of the enzyme, falling into two broad families, have been described based on sequence alignments (1), each differing in its selectivity for oxidizing substrates. The family 1A enzymes are soluble enzymes containing FMN as the only prosthetic group and use fumarate as the oxidizing substrate (2). The family 1B enzymes are soluble and, in addition to a subunit that resembles the family 1A enzyme, have a second protein subunit that contains an iron–sulfur center and an FAD (3); this electron transport chain reduces the physiological oxidant, NAD. The family 2 enzymes are membrane-bound enzymes that contain FMN and are oxidized by ubiquinone (4). The majority of eukaryotes and Gram negative bacteria have family 2 DHODs.

Scheme 1



In all DHODs, DHO is oxidized by the enzyme-bound FMN prosthetic group to form the α,β -unsaturated carbonyl moiety of the product orotate (Scheme 1). Oxidations that form α,β -unsaturated carbonyl compounds are catalyzed by a number of flavin-containing enzymes (5). In such oxidation reactions, the somewhat acidic proton α to the carbonyl [in this case, the C5 *pro S* hydrogen of DHO (6)] is removed by an enzymatic base and the β -hydrogen (in this case, the hydrogen on C6 of DHO) is transferred as a hydride to the isoalloxazine of the flavin. These two hydrogens may be transferred in a single step (a concerted reaction), or substrate deprotonation may precede hydride transfer (a stepwise reaction). From isotope effects on the steady-state kinetics of the reaction catalyzed by the family 1A DHOD from *Crithidia fasciculata*, it was concluded that proton abstraction and hydride transfer to FMN occurred in steps (6). Similar studies on the family 2 DHOD from bovine liver suggested a concerted mechanism for DHO oxidation (7), as did studies on the family 1B enzyme from *Clostridium oroticum* (8). Thus, it appears that the reaction mechanism is imposed by the protein rather than by the requirements of FMN and DHO.

[†] Supported by grants from the Danish National Science Council and the Carlsberg Foundation. B.A.P. supported by grants from the NIH to David P. Ballou and Vincent Massey (GM 20877 to D.P.B., GM 11106 to V.M.).

^{*} To whom correspondence should be addressed. E-mail: brupalf@umich.edu. Phone: (734) 763-2449. Fax: (603) 687-1852.

[‡] University of Michigan.

[§] University of Copenhagen.

¹ Abbreviations: CAPS, 3-(cyclohexylamino)propanesulfonic acid; DHOD, dihydroorotate dehydrogenase; DHO, dihydroorotate; Tris-HCl, Tris-(hydroxymethyl)aminomethane hydrochloride; KPi, potassium phosphate buffer; NaPi, sodium phosphate buffer; OA, orotate.

DHODs from each family have been characterized structurally (refs 9–12; Nørager and Larsen, personal communication). The active sites where DHO binds and is oxidized are nearly identical in all of these structures. Structures of the product complexes show that orotate is held by a number of hydrogen bonds from asparagine side chains, a serine or threonine side chain, and several backbone amides. Additionally, there is a salt-bridge between the carboxylate of orotate and a lysine of the enzyme. Presumably, the enzyme makes analogous interactions with DHO prior to oxidizing this substrate (11). One important difference between the family 1 enzymes and the family 2 enzymes to emerge from sequence comparisons (1) and structural studies (refs 9, 12; Nørager and Larsen, personal communication) is that the active-site base of family 1 DHODs is cysteine, while the analogous residue in the enzymes from family 2 is serine. Thus, the identity of the base may be one factor that determines whether DHO will be oxidized in a stepwise reaction or in a concerted reaction.

To begin to address these mechanistic issues, we have studied the reduction of the family 2 DHOD from *Escherichia coli* by stopped-flow methods. The enzyme from *E. coli* is a monomer that is associated with the membrane in vivo, but is also soluble in water and forms oligomers in the absence of detergents (13). The significant sequence homology and structural similarity to human DHOD make the *E. coli* enzyme an excellent model for that important drug target. In rapid reaction studies, we have detected intermediates prior to and following flavin reduction. The pH dependence of the rate constant for reduction is consistent with the notion that Ser175 is activated by the enzyme to act as a base. Our kinetic results also demonstrate that there must be a quinone binding site that is separate from the DHO/orotate binding site, in agreement with the crystal structures, and that the quinone menadione, but not molecular oxygen, is an excellent oxidizing substrate.

EXPERIMENTAL PROCEDURES

DHOD from *E. coli* was prepared and purified from the strain SØ6645 transformed with pAG1 as described (13). Menadione was from Pfaltz and Bauer; other chemicals were from Sigma. Absorbance spectra were obtained on a Hewlett-Packard 8450a diode array spectrophotometer or a Shimadzu UV-2501PC scanning spectrophotometer. Enzyme solutions were made anaerobic in glass tonometers for rapid reaction studies by repeated cycles of evacuation and equilibration over an atmosphere of purified argon (14). Reactants were made anaerobic by bubbling solutions with purified argon within the syringes that were to be loaded onto the stopped-flow instrument. For oxygen-containing solutions, syringes containing buffer with or without orotate were bubbled at room temperature and atmospheric pressure with O₂/Ar mixtures. When reduced enzyme was required, a gastight syringe containing dithionite was attached to a tonometer equipped with a sidearm cuvette, and the anaerobic enzyme was titrated to complete reduction as judged spectrally. Stopped-flow studies were performed at 4 °C using either a Hi-Tech SF-61 instrument or a Kinetic Instruments stopped-flow spectrophotometer. The pH dependence of the reductive half-reaction was studied in two ways. At a few pH values spanning the range from 6 to 12.7, enzyme equilibrated with the buffer at the pH of interest was mixed with solutions of

DHO of various concentrations in the same buffer. The reduction rate constant was obtained from the limiting value of the observed rate constant extrapolated to infinite DHO concentration (15). Reduction rate constants were also obtained in pH jump experiments by mixing anaerobic oxidized enzyme in 5 mM Tris-HCl, pH 8.5, with 10 mM DHO in 0.1 M buffer solutions at the desired pH. The pH values of 1:1 mixtures of the concentrated buffers and 5 mM Tris-HCl, pH 8.5, were measured at 4 °C and used for the pH values of the reactions. The following concentrated buffers were used: 0.1 M KPi, pH 6.0–7.5; 0.1 M Tris-HCl, pH 7.5–9.5; 0.1 M glycine, pH 9.0–10.75; 0.1 M CAPS, pH 11.6–11.7; 0.1 NaPi, pH 12–12.7. Control experiments demonstrated that the enzyme equilibrated rapidly with the new pH of the solution after mixing. Observed rate constants were obtained by fitting single reaction traces to sums of exponentials using the data collection software. Alternatively, traces obtained at a particular concentration of DHO but at different wavelengths were simultaneously fit to the same set of observed rate constants using the programs Scientist (MicroMath) or pro Fit (Quantum Soft). The pK_a values controlling the reduction rate constant and the dissociation constant of DHO were obtained by fitting the pH dependence to eqs 1 and 2,

$$k_{\text{red}}^{\text{obs}} = k_{\text{red}}^{\text{max}} \left(\frac{10^{-\text{p}K_{\text{a}}}}{10^{-\text{p}K_{\text{a}}} + 10^{-\text{pH}}} \right) \quad (1)$$

$$K_{\text{d}}^{\text{obs}} = K_{\text{d}} \left(1 + \frac{10^{-\text{p}K_{\text{a}}}}{10^{-\text{pH}}} \right) \quad (2)$$

respectively, using pro Fit. The reduction potential of the enzyme-bound flavin was determined spectrophotometrically at 25 °C in 0.1 M KPi, pH 7.0, by the xanthine/xanthine oxidase method of Massey (16). 8-Aminoriboflavin (*E*_{m7} = –330 mV) was used as the redox indicator dye.

RESULTS

Reaction Intermediates in the Reduction of DHOD by DHO. The reduction of the enzyme-bound FMN by DHO was observed directly by mixing anaerobic solutions of DHOD with anaerobic solutions of DHO in a stopped-flow apparatus at 4 °C. The absorbance spectra of the species involved in this reaction at pH 8.5 were calculated from traces obtained at intervals from 320 to 650 nm. DHO binding to DHOD was complete within the dead-time of the instrument (~1 ms) and caused a large red shift in the oxidized flavin absorbance spectrum (Figure 1). This ~20 nm shift in the major flavin absorbance peak for the transient enzyme–substrate complex is similar to the spectral changes previously observed for orotate complexes of both the *E. coli* enzyme and the family 1A enzymes from *Lactobacillus lactis* and *Enterococcus faecalis* (1, 17, 18).

Three reaction phases were observed following the formation of the enzyme–substrate complex (Figure 2). The first of these, reduction of FMN by DHO, was accompanied by a decrease in absorbance between 340 and 530 nm and an increase from 530 to 650 nm to form the second intermediate on the reaction pathway, the reduced enzyme–orotate complex. The observed rate constant for this reaction increased with DHO concentration to a limiting value of 45.7

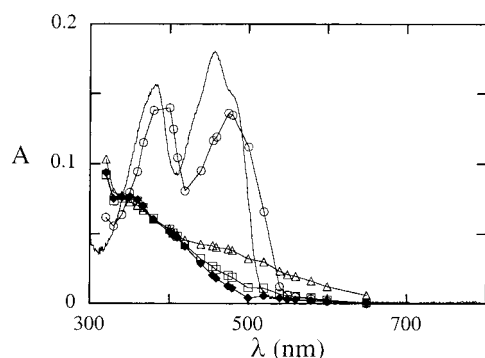


FIGURE 1: Spectra of reaction intermediates. Anaerobic DHOD ($\sim 14 \mu\text{M}$ active sites) was mixed with anaerobic DHO (20 mM) in 0.1 M Tris-HCl buffer, pH 8.5, at 4°C in a stopped-flow spectrophotometer. Reaction traces were collected from 320 to 650 nm and fit to the sum of three exponentials. The amplitudes were used to construct the spectra of intermediates (data points). The spectrum of the free oxidized DHOD was obtained in the stopped-flow instrument by mixing the free enzyme with anaerobic buffer (solid line). The spectrum of the DHOD–DHO complex that developed in the dead-time of the instrument (~ 1 ms) is marked with circles. Reduction of the flavin by DHO formed the reduced enzyme–orotate charge-transfer complex marked with triangles. The slow dissociation of orotate from the enzyme resulted in the spectrum marked by the squares, which very slowly converted to the final reduced enzyme spectrum marked with diamonds.

$\pm 0.3 \text{ s}^{-1}$ at pH 8.5. The K_d of DHO was determined from its half-saturating concentration as $20 \pm 1 \mu\text{M}$ (15). The reduced enzyme–orotate complex produced by this reaction was characterized by an additional broad absorbance band centered near 500 nm (Figure 1), characteristic of a reduced flavin–orotate charge-transfer complex. Such charge-transfer absorbances are the result of the excitation of electrons from the orbitals of an electron-rich donor (reduced FMN) into the orbitals of an electron-deficient acceptor (orotate), and require the proper alignment of the charge-transfer pair. Thus the charge-transfer band is consistent with the stacked arrangement of isoalloxazine and orotate that would be expected from the structures of the oxidized DHOD–orotate complexes that have been determined crystallographically (10–12).

The loss of the charge-transfer absorbance occurred in the second reaction phase (Figures 1 and 2C). The extent of orotate loss from this complex depended on the concentration of DHO present in the experiment. At high DHO concentrations, little charge-transfer absorbance remained, while at low DHO concentrations, significant amounts of orotate remained bound to the enzyme. This observation suggests that orotate binds tightly to the reduced enzyme and that a competing ligand such as DHO is required to drive the dissociation of the charge-transfer complex. This situation results in a decrease in the observed rate constant as the concentration of the trapping ligand (DHO) increases and drives the reaction further (Figure 3B), similar to the mechanism analyzed for xanthine dehydrogenase (20). A limiting value of 0.32 s^{-1} was obtained at pH 8.5. The events of the second reaction phase are summarized by the last two reactions of Scheme 2. The dissociation of orotate from the reduced enzyme is too slow to be on the catalytic cycle (see below), indicating that the free reduced enzyme is not a catalytically competent intermediate.

As discussed below, orotate binds to the reduced enzyme with a K_d of 64 nM. In order for DHO to compete effectively

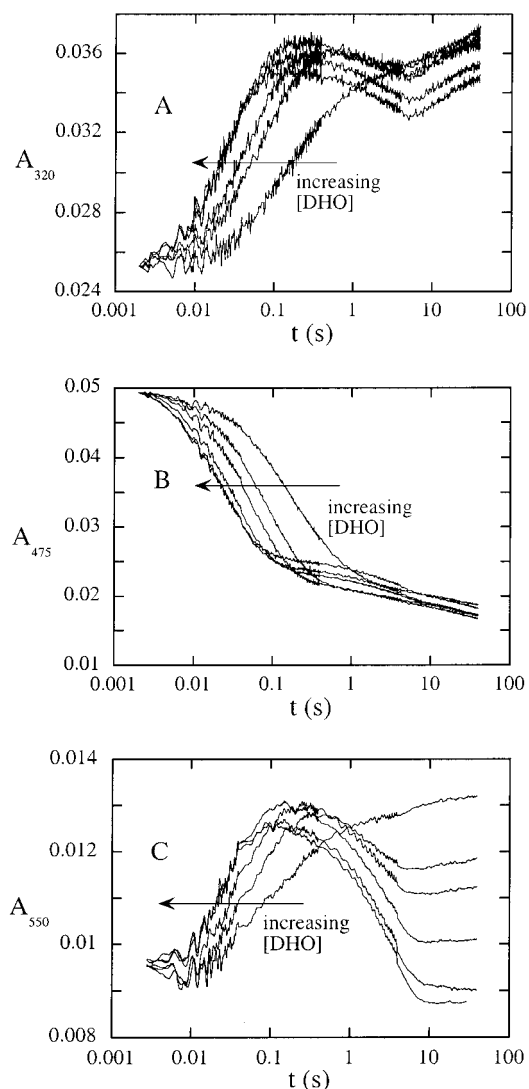


FIGURE 2: Reduction of DHOD observed at selected wavelengths. Anaerobic DHOD (final concentration of $\sim 4 \mu\text{M}$ in active sites) was mixed with various concentrations of anaerobic DHO (138, 69, 34.5, 6.9, and $3.4 \mu\text{M}$ after mixing) in 0.1 M Tris-HCl buffer, pH 8.5, at 4°C in a stopped-flow spectrophotometer. Note that the reaction traces are displayed on a logarithmic time scale and have been adjusted to identical starting absorbances to facilitate comparison. Reduction of the red-shifted DHOD–DHO complex was seen in the first phase as an increase in absorbance at 320 nm (A), a decrease at 475 nm (B), and an increase at 550 nm (C).

with orotate, it must also bind tightly to the reduced enzyme. In the presence of the $\sim 4 \mu\text{M}$ orotate produced by enzyme reduction, an apparent dissociation constant of $\sim 10 \mu\text{M}$ for DHO was estimated from the absorbance remaining after the charge-transfer complex equilibrated with DHO (Figure 3C). This apparent K_d is a function of the K_d values of both DHO and orotate and the concentration of free orotate. The absorbance is the sum of the concentrations of the charge-transfer complex, the free reduced enzyme, and the reduced enzyme–DHO complex multiplied by their respective extinction coefficients. The concentrations of these species are governed by the dissociation constants of orotate and DHO from the reduced enzyme and were calculated using the method of Storer and Cornish-Bowden (21) fixing the K_d value of 64 nM for orotate (see below), the total enzyme concentration to $4 \mu\text{M}$, and the total orotate concentration to $4 \mu\text{M}$. The K_d value for DHO was found by minimizing

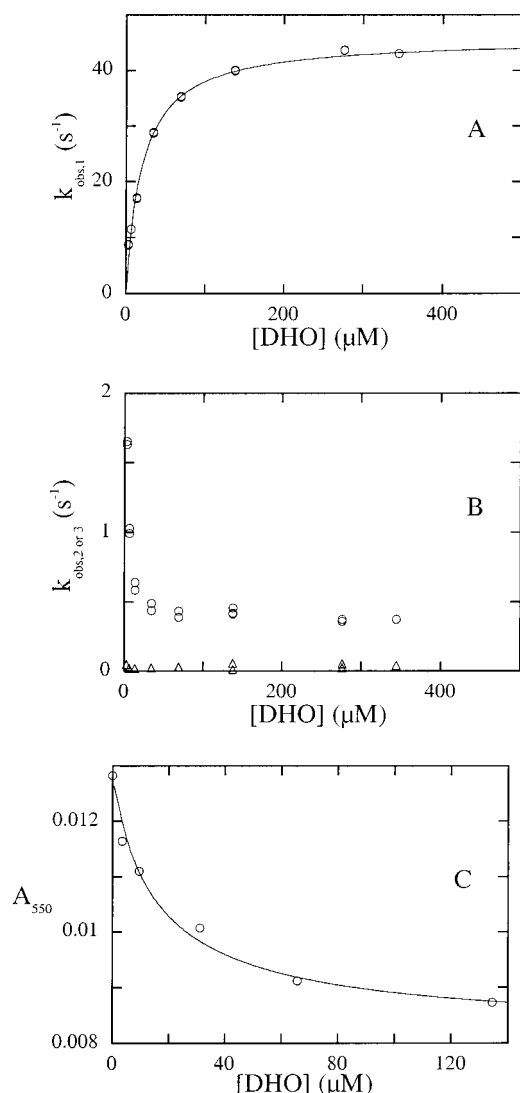
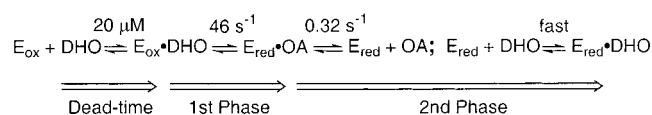


FIGURE 3: Concentration dependence of observed rate constants in the reaction of DHOD and DHO. Stopped-flow traces obtained at pH 8.5 and 4 °C such as those in Figure 2 were fit to the sum of three exponentials, and the observed rate constants (k_{obs}) for each phase were plotted as a function of DHO concentration. (A) The values for the first reaction phase (flavin reduction) saturated to a limiting rate constant of 46 s^{-1} . A value of 20 μM was obtained for the K_d from the half-saturating concentration of DHO. (B) The observed rate constants for orotate dissociation from the charge-transfer complex are shown by circles, and the observed rate constants for the final small phase are shown by triangles. (C) The absorbance remaining after the end of the second phase as a function of DHO concentration was fit as described in the text to obtain an estimate of the K_d for DHO of $0.2 \pm 0.1 \mu\text{M}$.

Scheme 2



the difference between the calculated and experimental absorbance data using the Levenberg–Marquardt algorithm in a fitting module in pro Fit (for source code of the fitting module, see Supporting Information). A value of $200 \pm 100 \text{ nM}$ for the K_d of DHO to free reduced enzyme was found which is about 100-fold tighter than when the enzyme is oxidized. In a separate experiment, the binding of DHO to the free reduced enzyme was demonstrated directly by

reducing anaerobic DHOD with the xanthine/xanthine oxidase reducing system and recording the change to the absorbance spectrum that occurred upon addition of DHO (data not shown). Absorbance changes were evident confirming the formation of a reduced enzyme–DHO complex, with increases in absorbance from 340 to 370 nm (difference maximum at 356 nm) and 385 to 460 nm (difference maximum at 420 nm). These increases were too small to allow the direct measurement of the dissociation constant.

A third, very slow reaction phase was observed at 475 nm. The observed rate constant of this reaction ($\sim 0.02 \text{ s}^{-1}$) did not vary with DHO concentration or pH, and the amplitude of the absorbance change of this reaction was small. At this time, it is not possible to assign this spectral change to a chemical or physical process. Possibilities include the dissociation of aggregated enzyme (13), a slow conformational change, or the reaction of some damaged enzyme. Regardless of its origin, this reaction is much too slow to be catalytically relevant.

pH Dependence of the Reaction between DHO and DHOD. As described in Experimental Procedures, the kinetics of the reductive half-reaction were examined as a function of pH in anaerobic stopped-flow experiments in two ways. In the first method, enzyme at the pH of the experiment was mixed with a range of concentrations of DHO at the same pH in order to obtain both the limiting rate constant for reduction and the K_d of DHO (15). Alternatively, the limiting rate constant for reduction was obtained in pH-jump reduction experiments, in which anaerobic enzyme in 5 mM Tris-HCl, pH 8.5, was mixed with saturating DHO solutions in 100 mM buffer at a different pH. Control experiments gave identical results by both methods, indicating that the acid/base groups of the active site of the oxidized enzyme equilibrated rapidly with the solution. The rate constant for hydride transfer was determined at saturating DHO concentrations from pH 6 to 12.7. It increased with increasing pH until a limiting value of $360 \pm 20 \text{ s}^{-1}$ was reached above a $\text{p}K_a$ of 9.5 ± 0.1 (Figure 4A). This $\text{p}K_a$ belongs to a group in the oxidized enzyme–DHO complex which we tentatively assign to the active-site base, Ser175. At all pH values where the enzyme was stable, the observed rate constant for flavin reduction increased hyperbolically with DHO concentration (Figure 3). The binding affinity of DHO was essentially independent of pH up to pH 10 ($K_d = 14 \pm 3 \mu\text{M}$), and then increased with pH, reaching a value of 4 mM at pH 12.7 (the highest pH value where the enzyme was stable; Figure 4B). This increase in the K_d could be due to the ionization of the N3 proton of DHO and consequent depletion of the N3 protonated form at high pH. The value of this $\text{p}K_a$ has been reported as 11.46 at an ionic strength of 1.0 M at 25 °C (19). Alternatively, the increase in K_d at high pH may be due to the deprotonation of Lys66 which forms a salt bridge to orotate in the product complex (Nørager and Larsen, personal communication) and presumably forms a similar interaction in the DHO complex. Our data fit with a $\text{p}K_a$ of 10.3 ± 0.1 .

Oxidation of Reduced DHOD by Orotate. Anaerobic DHOD at pH 8.5 was reduced by titrating with dithionite, and this solution was mixed with anaerobic orotate solutions in a stopped-flow spectrophotometer. At orotate concentrations higher than 110 μM , the reduced DHOD–orotate charge-transfer complex formed in the dead-time of the

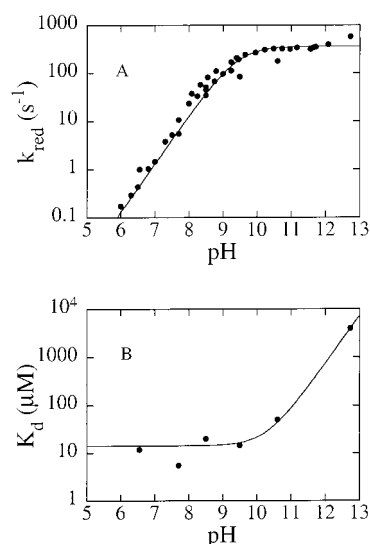


FIGURE 4: pH dependence of DHOD reduction. (A) The limiting rate constants for reduction (k_{red}) were obtained by either repeating the analysis described for Figure 3A for data collected at different pH values or from pH-jumps with saturating DHO as described in the text. The curve represents a fit of eq 1 to the data. (B) The observed dissociation constants for DHO were obtained at different pH values from the variation of the observed rate constants with DHO concentration. The curve represents a fit to eq 2.

stopped-flow instrument (Figure 5). At the lowest orotate concentrations (25–110 μM), the formation of the charge-transfer complex was slow enough to be observed. The observed rate constant for this phase varied linearly with orotate concentration, giving an estimate of $5 \times 10^6 \text{ M}^{-1} \text{ s}^{-1}$ for the bimolecular association rate constant. The orotate dissociation rate constant determined in studies of the reaction of DHO with oxidized DHOD described above was 0.32 s^{-1} , allowing the K_d for orotate to be estimated as $0.32 \text{ s}^{-1} / 5 \times 10^6 \text{ M}^{-1} \text{ s}^{-1} = 64 \text{ nM}$. A value of 5 μM for the dissociation constant of orotate from the oxidized enzyme had been measured at 25°C (13). We repeated that spectrophotometric titration at 4°C in 0.1 M Tris-HCl, pH 8.5, and found a value of 30 μM (data not shown). Therefore, when compared under identical conditions, orotate binds to the reduced enzyme nearly 500-fold more tightly than to the oxidized enzyme.

A second reaction phase was associated with an increase in absorbance at 475 nm and a loss of charge-transfer absorbance at 550 nm, representing flavin oxidation by orotate. The observed rate constant decreased with increasing orotate concentration, reaching a limiting value of 0.032 s^{-1} . The decrease of the observed rate constant with increasing reactant concentration indicates that at least one unimolecular reaction precedes the bimolecular step, and at high concentrations, the unimolecular step becomes rate determining (20). In the present case, the second reaction phase is composed of flavin oxidation by orotate, DHO dissociation, and binding of orotate (Scheme 3). At high orotate concentrations, the rate constant for the overall process is determined by the hydride transfer reaction from FMN to orotate. A third, very slow ($<0.01 \text{ s}^{-1}$), small absorbance increase was observed at 475 nm at the lowest orotate concentrations. We are unable to assign this reaction to a chemical or physical process.

The data from the forward reaction (enzyme reduction by DHO) and the reverse direction (enzyme oxidation by

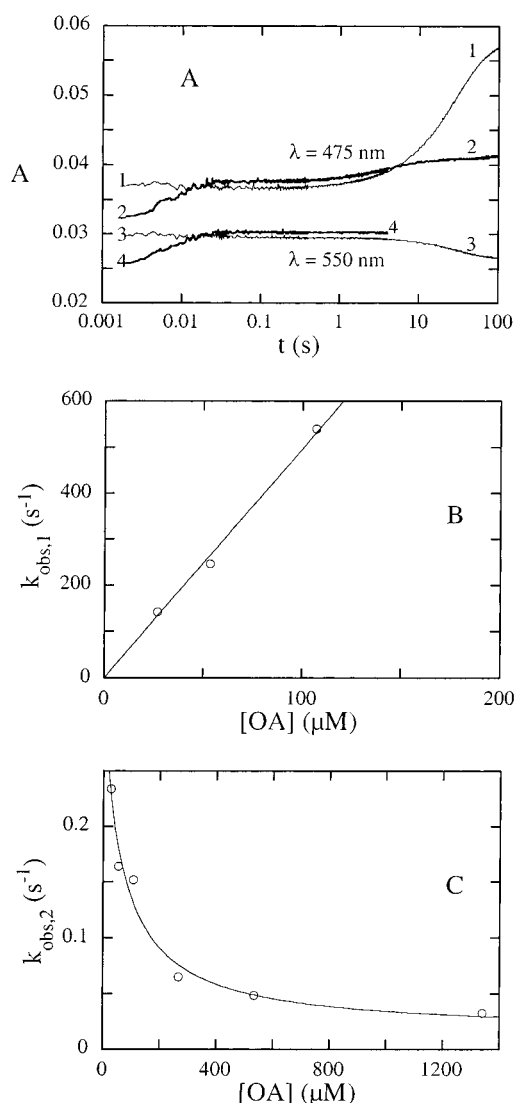
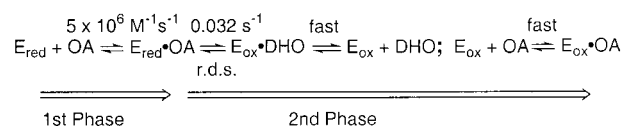


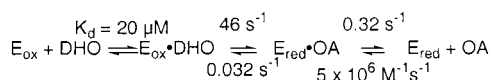
FIGURE 5: DHOD oxidation by orotate. The reverse of the reductive half-reaction was studied by mixing dithionite-reduced DHOD with anaerobic orotate solutions in 0.1 M Tris-HCl, pH 8.5, at 4°C in a stopped-flow spectrophotometer. (A) Representative reaction traces are shown from two extremes of orotate concentration at wavelengths sensitive to oxidized flavin (475 nm) and the reduced enzyme–orotate charge-transfer complex (550 nm). Note that the reaction traces are displayed on a logarithmic time scale. Curve 1 shows the absorbance at 475 nm using 1.34 mM orotate after mixing. Curve 3 is the same reaction observed at 550 nm. Curve 2 shows the absorbance at 475 nm using 27 μM orotate after mixing, and curve 4 is the same reaction observed at 550 nm. Panel B shows the concentration dependence of the first observed rate constant ($k_{\text{obs},1}$) (slope = $5 \times 10^6 \text{ M}^{-1} \text{ s}^{-1}$) and panel (C) shows the concentration dependence of the second observed rate constant ($k_{\text{obs},2}$).

Scheme 3



orotate) are combined in Scheme 4 which shows the rate constants of the reductive half-reaction at pH 8.5 and 4°C . We find an internal equilibrium constant for FMN reduction by DHO of 1400, which is equivalent to a ΔG° of $-4.0 \text{ kcal mol}^{-1}$.

Scheme 4



Midpoint Potential. The midpoint potential of the enzyme-bound FMN was determined using the xanthine/xanthine oxidase method at 25 °C, pH 7.0, to be −310 mV (data not shown). This value is 103 mV lower than free FMN, indicating that the enzyme binds the reduced flavin less tightly than it binds the oxidized flavin by a factor of 3000.

Oxidation of Reduced DHOD by Menadione. Respiratory quinones are thought to be the physiological oxidants of *E. coli* DHOD. Menadione, which has a higher solubility in water than ubiquinone, was used as a convenient model quinone substrate to study the oxidation of the reduced enzyme at pH 8.5 and 4 °C. Dithionite-reduced DHOD was mixed with anaerobic solutions of the quinone in the stopped-flow spectrophotometer. DHOD was oxidized by menadione in a biphasic reaction, with the largest absorbance change occurring at 456 nm (data not shown). The first reaction phase consisted of ~90% of the absorbance change. The observed rate constant for this phase increased hyperbolically with menadione concentration to a limiting value of $180 \pm 30 \text{ s}^{-1}$. The K_d for menadione determined from the half-saturating concentration was $110 \pm 20 \mu\text{M}$. The second reaction phase, representing ~10% of the total absorbance change, was slower than the first phase ($120 \pm 30 \text{ s}^{-1}$) and also increased hyperbolically with menadione concentration, with a half-saturation concentration of $500 \pm 200 \mu\text{M}$. There were no absorbance changes at long wavelengths (550 and 600 nm). Thus we could not detect any menadione charge-transfer or semiquinone intermediates.

As described above, orotate dissociates from reduced DHOD too slowly to be catalytically relevant. This finding requires the oxidizing substrate to rapidly oxidize the reduced DHOD–orotate complex. Therefore we were interested in determining the kinetics of the reaction of menadione with the reduced DHOD–orotate complex. To accomplish this, free dithionite-reduced DHOD was mixed with solutions containing various concentrations of menadione and 1.2 mM orotate (after mixing). On the basis of our results for the oxidation of the enzyme by orotate (see above), the pseudo-first-order rate constant for orotate association under these conditions is 6000 s^{-1} , while oxidation by orotate is slow (0.032 s^{-1}). As predicted by these considerations, the reduced enzyme–orotate charge-transfer complex formed in the dead-time of the stopped-flow instrument. Complex formation was followed by a biphasic oxidation of the flavin by menadione. In the presence of orotate, the maximum absorbance increase caused by quinone oxidation occurred at 475 nm due to the large spectral perturbation to the oxidized flavin spectrum caused by orotate. The first reaction phase (Figure 6) constituted the majority of the absorbance change (~90%), and the observed rate constant varied hyperbolically with menadione concentration, giving a limiting oxidation rate constant of $180 \pm 8 \text{ s}^{-1}$ and a K_d of $43 \pm 7 \mu\text{M}$. The second reaction phase, representing ~10% of the total absorbance change, was about an order of magnitude slower than the first phase ($16 \pm 6 \text{ s}^{-1}$) and remained constant with menadione concentration. Thus, it is apparent that the majority of the reduced enzyme–orotate complex reacts

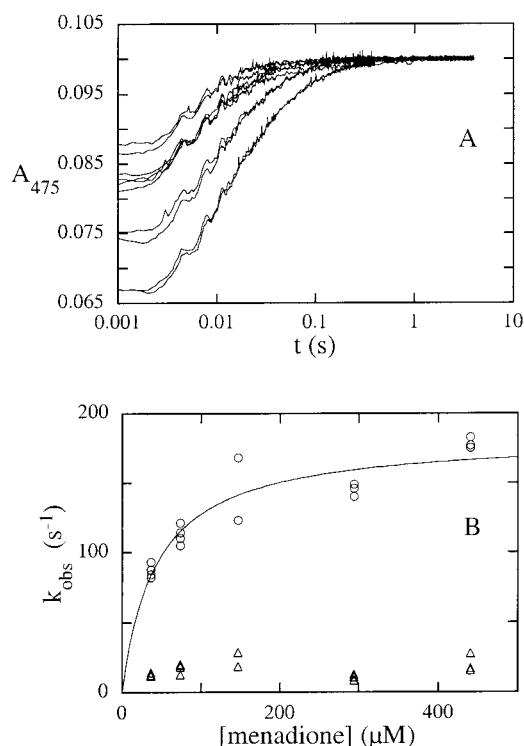


FIGURE 6: Oxidation of the reduced enzyme–orotate complex by menadione. Dithionite-reduced enzyme was mixed with anaerobic solutions of menadione containing orotate (1.2 mM after mixing). All solutions were in 0.1 M Tris-HCl, pH 8.5, and reactions were at 4 °C. (A) Reaction traces at the peak of oxidized flavin absorbance displayed on a logarithmic time scale. Menadione concentrations after mixing were 25, 50, 100, and 300 μM . (B) The concentration dependence of the first observed rate constant (circles) of the curves in panel A gave a limiting oxidation rate constant of $180 \pm 8 \text{ s}^{-1}$ and a K_d for menadione of $43 \pm 7 \mu\text{M}$. The observed rate constant of the second phase (triangles) was essentially constant with menadione concentration at $16 \pm 6 \text{ s}^{-1}$.

nearly as rapidly with menadione as the free reduced enzyme, providing direct confirmation that the reduced enzyme–orotate complex is a catalytically competent intermediate in the reaction with oxidants.

Oxidation of Reduced DHOD by O_2 and Ferricyanide. A variety of substrates will serve as the oxidizing substrate for DHOD, including molecular oxygen, and consequently DHOD has often been referred to as “dihydroorotate oxidase”. We investigated the kinetics of the reaction of reduced DHOD with O_2 at pH 8.5 and 4 °C, by mixing a solution of the dithionite-reduced enzyme with buffer solutions containing various concentrations of O_2 in the stopped-flow instrument. A plot of the pseudo-first-order rate constant vs the O_2 concentration was linear (data not shown), giving a bimolecular rate constant for oxidation of $6.2 \times 10^4 \text{ M}^{-1} \text{ s}^{-1}$. Including orotate in the oxygen syringe (1.2 mM after mixing) allowed the kinetics of the reaction of the reduced enzyme–orotate complex with O_2 to be determined, since orotate binding is rapid (see above) compared to the reaction of the free reduced enzyme with O_2 (6000 s^{-1} at 1.2 mM orotate vs 40 s^{-1} at the highest O_2 concentration used). The reaction of the reduced enzyme–orotate complex was also bimolecular with O_2 , but the rate constant, $5.0 \times 10^3 \text{ M}^{-1} \text{ s}^{-1}$, was an order of magnitude lower. Thus bound orotate provides some protection to the reduced enzyme from reaction with molecular oxygen.

The reaction of 15 μM dithionite-reduced enzyme with $\text{Fe}(\text{CN})_6^{3-}$, an obligate 1-electron acceptor, was also studied at pH 8.5 and 4 °C in anaerobic stopped-flow experiments by monitoring the increase in flavin absorbance at 480 nm where it was not obscured by $\text{Fe}(\text{CN})_6^{3-}$ absorbance. The free reduced enzyme reacted very rapidly, and at most concentrations of $\text{Fe}(\text{CN})_6^{3-}$ the reaction was essentially complete in the dead-time of the instrument. At the lowest $\text{Fe}(\text{CN})_6^{3-}$ concentration investigated that still maintained pseudo-first-order conditions (50 μM), an exponential increase in flavin absorbance was observed (not shown) which gave an apparent rate constant of 490 s^{-1} , allowing a second-order rate constant of $9.8 \times 10^6 \text{ M}^{-1} \text{ s}^{-1}$ to be estimated. No changes in absorbance were detected at 580 nm, where neutral flavin semiquinone absorbs.

The effect caused by the presence of orotate on $\text{Fe}(\text{CN})_6^{3-}$ oxidation was examined by including a high concentration of orotate (1.8 mM after mixing) in the syringe containing up to 200 μM $\text{Fe}(\text{CN})_6^{3-}$. Under these conditions, more than 80% of the reduced enzyme should bind orotate before reacting with $\text{Fe}(\text{CN})_6^{3-}$, because a pseudo-first-order rate constant of 9000 s^{-1} is expected for orotate binding, compared to an estimated limit for the reaction of free enzyme with 200 μM $\text{Fe}(\text{CN})_6^{3-}$ of $\sim 2000 \text{ s}^{-1}$. The absorbance at 480 nm increased in two phases of roughly equal amplitudes (data not shown). The observed rate constants of both phases varied linearly with $\text{Fe}(\text{CN})_6^{3-}$ concentration, giving bimolecular rate constants of $3.6 \times 10^5 \text{ M}^{-1} \text{ s}^{-1}$ and $3.2 \times 10^4 \text{ M}^{-1} \text{ s}^{-1}$. Thus the presence of orotate at the active site slowed flavin oxidation, but even with the ligand bound, the reaction was relatively rapid. The origin for the two reaction phases is not known. However, with the pyrimidine binding site blocked by orotate, the only avenue of approach for $\text{Fe}(\text{CN})_6^{3-}$ to reduced FMN is through the hydrophobic tunnel formed by the protein N-terminus that is thought to form the quinone binding site and normally would be attached to the cell membrane. It is worth noting that deletion of 5–40 residues of the protein N-terminus eliminates the ability of the enzyme to utilize quinones as substrates (Jensen, unpublished material), supporting the suggestion that it is the site for quinone binding. The dimers and higher-order aggregation states of the *E. coli* enzyme that have been detected in solution are probably due to intermolecular hydrophobic interactions in this region of the protein. It is possible that such interactions restrict access of $\text{Fe}(\text{CN})_6^{3-}$ to the hydrophobic tunnel and FMN. Thus we suggest that the two phases of enzyme oxidation represent monomeric and aggregated (dimeric or higher order) association states.

Enzyme-Monitored Turnover. The turnover number of the enzyme at pH 8.5 and 4 °C was estimated using menadione as the oxidizing substrate by monitoring the enzyme absorbance in the steady state. An anaerobic solution of DHOD was mixed in a stopped-flow instrument with anaerobic solutions containing DHO and menadione (6.9 μM DHOD, 1 mM DHO, and 200 μM menadione after mixing). Reactions were monitored at 475 nm and the turnover number was estimated from the area under the curve during the steady-state portion of the reaction. A turnover number of 19.7 s^{-1} was found. The high turnover number is incompatible with orotate dissociation from the reduced enzyme as part of the catalytic cycle.

DISCUSSION

Reductive Half-Reaction. The pH dependence of steady-state turnover by DHOD has been examined in detail for the family 2 enzyme from bovine liver (7), the family 1A enzyme from yeast (23), and the family 1B enzyme from *C. oroticum* (8). The k_{cat} values of both the family 1B and family 2 enzymes exhibited bell-shaped pH dependencies with maxima near 8.0, and a pK_a of about 7 was measured for groups that must be deprotonated for efficient catalysis. A similar pK_a value was determined for the family 1A enzyme. In each case, the pK_a value was ascribed to the active-site base, which is cysteine in both family 1 enzymes and serine in the family 2 enzyme. It is interesting to note that the pK_a values determined by steady-state kinetics all have similar values and are significantly lower than the value we obtained (9.5) by our more direct rapid reaction methods. Because k_{cat} depends on steps from the whole catalytic cycle, it is possible that the steady-state values are distorted from kinetic complexity. Alternatively, the differences in pK_a between the value we determined for the *E. coli* enzyme and these other enzymes could merely be the coincidental difference between the properties of enzymes from different species.

The oxidation of DHO to orotate by DHOD requires the participation of an enzymatic base. Mapping the sequence of the DHOD from *E. coli* onto the *L. lactis* structure has identified serine 175 as the base in *E. coli* DHOD (13). This assignment has been corroborated by the behavior of the Ser175Ala mutant, which has less than 0.01% of the activity of the wild type enzyme (13), and more recently verified by the crystal structure of the *E. coli* (Nørager and Larsen, personal communication) and homologous human (12) enzymes. Because the pK_a of an unperturbed serine hydroxyl is ~ 15 , very little of the required serine alkoxide would be present at physiological pH unless the protein structure significantly alters the pK_a to increase the proportion of alkoxide available for reaction. Our results demonstrate that FMN reduction by DHO is controlled by an enzyme group with an apparent pK_a of 9.5, and that the maximum rate constant for flavin reduction is 360 s^{-1} . If the rate constant for DHO dissociation from the red-shifted Michaelis complex is much larger than 360 s^{-1} , then DHO is in rapid equilibrium with the enzyme, and the observed pK_a controlling flavin reduction is an intrinsic pK_a . Alternatively, if the protonation state of the Michaelis complex is not at equilibrium with the solution (which could happen if DHO dissociation has a rate constant similar to or lower than that of flavin reduction, making DHO “sticky”), the observed pK_a would not represent an intrinsic value.

In the simplest scenario, we can assign this pK_a to serine 175. If DHO binding is in rapid equilibrium, then this pK_a is the intrinsic pK_a of serine 175 in the Michaelis complex, suggesting that the enzyme lowers the pK_a of this residue by ~ 5.5 units compared to the value of free aqueous serine, a relative stabilization of the alkoxide form of 7.7 kcal mol^{-1} . The origin of this stabilization is not clear. The crystal structure of the human DHOD shows that the analogous serine residue forms a hydrogen bond with a water molecule which makes a hydrogen bond to a threonine and a van der Waals contact with the face of the aromatic ring of a phenylalanine side chain (12). A similar network has been observed in the *E. coli* enzyme (Nørager and Larsen, personal

communication). Thus, at low pH values serine 175 can be envisioned as a component in a proton relay system. None of the components of this proton relay system appear to provide the significant electrostatic stabilization that would be needed to lower the pK_a of the active-site serine. However, it is worth noting that the crystal structures of the family 2 DHODs were obtained at pH values well below the experimentally observed pK_a value, allowing the possibility that the serine alkoxide is stabilized by interactions formed after a protein conformational change.

While there is a catalytic advantage in lowering the pK_a of the active-site base to a value that allows a significant amount of the reactive deprotonated form to be present, this advantage is offset by its lower reactivity as a base. In *E. coli* DHOD, Ser175 must remove the *pro S* proton from C5 of DHO, whose pK_a value in aqueous solution has been estimated as ~ 20 (24). If the pK_a of DHO is not perturbed upon binding to the enzyme, then this represents a 14.7 kcal mol⁻¹ barrier to the proton transfer from DHO to Ser175. Interactions between the enzyme and DHO—in particular, hydrogen bonds to the C4 carbonyl oxygen of DHO—can be expected to lower the pK_a of DHO if they become strengthened upon generating the negatively charged enolate of the deprotonated DHO. However, these interactions might not be enough to lower the pK_a of DHO by the ~ 10 units needed to match Ser175. In such a situation, DHO will not be deprotonated until the C5–H bond becomes significantly more polarized and weakened as the hydride of C6 is transferred to FMN, perhaps leading to a concerted β -hydride transfer and α -deprotonation as reported for the bovine DHOD, another family 2 DHOD (7).

It is not clear how DHOD promotes the transfer of the substrate hydride to FMN. DHO bound to the enzyme is likely to be held by a number of hydrogen bonds in an orientation that is roughly parallel to the isoalloxazine, with C6 of DHO in van der Waals contact with N5 of the flavin. It is clear from the large spectral change caused to the flavin by DHO binding that the electronic structure of the oxidized flavin has been significantly perturbed. The cause of this perturbation is not known, but it is very similar to the perturbation caused by orotate binding to oxidized DHOD from both *E. coli*, *L. lactis*, and *E. faecalis* (1, 17, 18). It has been suggested that this spectral shift is due to aromatic stacking interactions (1, 18). However, because the binding of DHO—a nonaromatic molecule—causes the same shift, this cannot be the explanation. It is not yet possible to offer more than speculative hypotheses on the cause of this large spectral shift. It is intriguing that the spectral shift occurs in the Michaelis complex prior to flavin reduction and not only in dead-end complexes. The large spectral shift clearly indicates a change in the electronic and/or vibrational structure of the isoalloxazine; this may be linked to enhanced chemical reactivity.

The midpoint potential of the orotate/DHO couple is -258 mV (25). We determined a value for the two electron potential of the ligand-free enzyme of -310 mV. Thus, DHO is not a sufficiently strong reducing agent to produce free reduced enzyme. Instead, the reaction is driven to the reduced flavin–orotate complex by a substantial increase in the affinity of the enzyme for its pyrimidine ligand upon flavin reduction. This increase in affinity is reflected in the very tight binding of orotate ($K_d = 64$ nM) to the reduced enzyme.

Therefore, from a thermodynamic viewpoint, *E. coli* DHOD drives flavin reduction through a strengthening of protein–ligand interactions, but these interactions prevent the dissociation of the product orotate, and the reduced enzyme–orotate complex must be oxidized by the oxidizing substrate ubiquinone. This situation is similar to that reported for acyl CoA dehydrogenases, where flavin reduction is also driven by a tightening of ligand binding, preventing product dissociation prior to flavin oxidation by electron-transferring flavoprotein (26). *E. coli* DHOD also binds DHO more tightly when the flavin is in the reduced state. The available family 2 DHOD structures provide no obvious basis for the redox-dependent ligand binding strength or for the drastically diminished rate of orotate release upon flavin reduction. It is apparent from all DHOD structures that the conserved protein loop containing the active-site base must move in order to allow access to the active site by ligands. However, there are no direct interactions between this loop and the isoalloxazine of FMN so that other models are required to account for the redox-dependent protein dynamics. One possibility is that lysine 66 changes its environment upon flavin reduction. In oxidized enzyme–orotate crystal structures, the presumably cationic amino group of Lys66 forms hydrogen bonds to the carboxylate of orotate and the imine nitrogen (N5) of the isoalloxazine. Upon flavin reduction, N5 becomes an amine nitrogen and its preferred geometry as a hydrogen bond acceptor will be significantly different. This would weaken the hydrogen bond with Lys66, freeing the side chain to strengthen its hydrogen bond with orotate with only a slight movement. While such a strengthened hydrogen bond could account for the redox-dependent change in ligand dissociation constants, it is not clear if this would also result in the observed slow release of orotate, since carboxylate–lysine interactions are numerous in enzymology and have not been noted for being kinetically stable. It is possible that a change to the orotate–lysine hydrogen bond could be propagated to the loop covering the active site via changes in the carboxylate geometry.

Oxidative Half-Reaction. Because orotate is in contact with the reduced flavin as a charge-transfer complex, it is not possible for the quinone substrate to occupy the same binding site, so that a separate quinone binding site is required. This binding site has been identified crystallographically (12). Two mechanisms of flavin oxidation by quinones may be envisioned: direct hydride transfer from the flavin to the quinone, or two single-electron transfers through a substrate semiquinone–flavin semiquinone intermediate pair. In flavin hydride transfer reactions, N5 of the isoalloxazine moiety is the reaction site. Since orotate is bound over the *si*-face of the flavin (Nørager and Larsen, personal communication) as with the human DHOD (12) and DHOD A from *L. lactis* (11), a hydride transfer to a quinone would require that the opposite face of the flavin be accessible to quinones. However, the crystal structures demonstrate that the *re*-face of the flavin is not accessible to ligands, so that a significant conformational change would be necessary to enable a hydride transfer. The alternative mechanism, two single-electron transfer steps, is less demanding sterically. Single electron transfer reactions are possible over large distances, and a variety of orientations are known for electron-transfer reactions between flavins and other redox cofactors (5). Quinone reduction by flavins via single electron steps over

long distances has been detected in several enzymes, including NADH peroxidase, trypanothione reductase, and lipoamide dehydrogenase (27–29). In the present case, there was no direct spectral evidence for a di-radical intermediate. However, this does not rule out the possibility of a di-radical intermediate, but merely requires that the rate constant for the second electron transfer reaction be much greater than that of the first reaction. We tested the feasibility of forming a fleeting flavin semiquinone intermediate by studying the reaction of ferricyanide, an obligate one-electron oxidant. This reagent rapidly oxidized reduced DHOD. Such a reaction must proceed through a flavin semiquinone intermediate, but this intermediate was not detected spectrally, indicating that the oxidation of the semiquinone by ferricyanide was even faster than the rapid reaction of the oxidant with fully reduced enzyme. Therefore, single electron-transfer reactions from the enzyme are feasible.

When the active site of the reduced enzyme was occupied by orotate, the reactions with menadione, molecular oxygen, and ferricyanide were slower than for the free enzyme. Thus, orotate provides a degree of protection to the reduced flavin from oxidants. Protection by orotate may be most simply explained by assuming that there are two reaction channels available to these reagents in the free enzyme: over the face of the flavin in the empty orotate binding site, and from the quinone binding site. Orotate binding prevents the reaction at the former site, decreasing the observed rate constant, but has no effect on the reaction at the quinone binding site. The observed rate constant for the oxidation of the free enzyme represents the sum of the rate constants for the reactions at each site. When orotate blocks the pyrimidine site, only the rate constant for reaction at the quinone binding site is observed. Interestingly, both molecular oxygen and ferricyanide react an order of magnitude more slowly through the quinone binding site than through the orotate site, while there is less than a 2-fold difference when menadione is the oxidant. This suggests that menadione has similar reactivity at both sites. Similar reactivities at both sites would be unlikely if the reaction of menadione at one site were a hydride transfer, owing to the strict orientation dependence of hydride transfer reactions (30). Because superoxide is thought to be an intermediate in oxidations by O_2 , the hydrophobicity of the site of reaction of molecular oxygen has been suggested to be an important determinant in its reactivity with reduced flavoproteins (31). In the case of *E. coli* DHOD, it is likely that O_2 can react in the pyrimidine binding site or in the quinone binding site. Because the pyrimidine binding site is ringed with polar and cationic groups, it provides a more polar environment than the hydrophobic quinone binding site, resulting in a 10-fold higher oxidation rate when the pyrimidine site is available. Similar considerations could apply to the difference in reactivities of the two sites toward ferricyanide. The highly charged anion should be accommodated preferentially in the pyrimidine binding site. When this is blocked by orotate, then the ion must approach the reduced flavin through the largely hydrophobic quinone binding tunnel or react through a long-range electron-transfer mechanism.

An alternative to a two reaction-channel model described above is that the presence of orotate changes the inherent reactivity of the reduced flavin. We have shown that the presence of a pyrimidine ligand makes the flavin a better

oxidant, and, therefore, a thermodynamically less reactive reductant. This increase in flavin potential could cause a decrease in the rate that it donates electrons to an oxidizing agent. Orotate caused a ~ 2 -fold slowing of the rate of reaction by menadione and a ~ 10 -fold slowing of the reaction with both O_2 and $Fe(CN)_6^{3-}$, both of which presumably must form an intermediate flavin semiquinone. This suggests a similar reaction mechanism for the latter two reactants and that the charge-transfer interaction between the reduced flavin and orotate preferentially inhibits one-electron oxidation of the flavin.

ACKNOWLEDGMENT

We wish to thank Professors David P. Ballou and Vincent Massey, University of Michigan, for the generous use of their facilities, and Vincent Massey for his gift of xanthine oxidase and 8-aminoriboflavin.

SUPPORTING INFORMATION AVAILABLE

Source code for the pro Fit module used to fit the charge-transfer absorbance data in the determination of the K_d of DHO to the reduced enzyme in the presence of orotate. This material is available free of charge via the Internet at <http://pubs.acs.org>.

REFERENCES

1. Björnberg, O., Rowland, P., Larsen, S., and Jensen, K. F. (1997) *Biochemistry* 36, 16197–16205.
2. Nagy, M., Lacroute, F., and Thomas, D. (1992) *Proc. Natl. Acad. Sci. U.S.A.* 89, 8966–8970.
3. Nielsen, F. S., Andersen, P. S., and Jensen, K. F. (1996) *J. Biol. Chem.* 271, 29359–29365.
4. Jones, M. E. (1980) *Annu. Rev. Biochem.* 49, 253–279.
5. Palfey, B. A., and Massey, V. (1998) in *Comprehensive Biological Catalysis, volume III/Radical Reactions and Oxidation/Reduction* (Sinnott, M., Ed.) Chapter 29, pp 83–154, Academic Press.
6. Pascal, R. and Walsh, C. T. (1984) *Biochemistry* 23, 2745–2752.
7. Hines, V. and Johnston, M. (1989) *Biochemistry* 28, 1227–1234.
8. Argyrou, A., Washabaugh, M. W., and Pickart, C. M. (2000) *Biochemistry* 39, 10373–10384.
9. Rowland, P., Nielsen, F. S., Jensen, K. F., and Larsen, S. (1997) *Structure* 5, 239–250.
10. Rowland, P., Nørager, S., Jensen, K. F., and Larsen, S. (2000) *Structure* 8, 1227–1238.
11. Rowland, P., Björnberg, O., Nielsen, F. S., Jensen, K. F., and Larsen, S. (1998) *Protein Sci.* 7, 1269–1279.
12. Liu, S., Neidhardt, E. A., Grossman, T. H., Ocain, T., and Clardy, J. (2000) *Structure* 8, 25–33.
13. Björnberg, O., Grüner, A.-C., Roepstorff, P., and Jensen, K. F. (1999) *Biochemistry* 38, 2899–2908.
14. Williams, C. H., Jr., Arscott, D. L., Matthews, R. G., Thorpe, C., and Wilkinson, K. D. (1979) *Methods Enzymol.* 62, 185–198.
15. Strickland, S., Palmer, G., and Massey, V. (1975) *J. Biol. Chem.* 250, 4048–4052.
16. Massey, V. (1990) in *Flavins and Flavoproteins*. (Curti, B., Ronchi, S., and Zanetti, G., Eds.) pp 59–66, Walter de Gruyter, Berlin, Germany.
17. Larsen, J. N., and Jensen, K. F. (1985) *Eur. J. Biochem.* 151, 59–65.
18. Marcinkeviciene, J., Jiang, W., Locke, G., Kopcho, L. M., Rogers, M. J., and Copeland, R. A. (2000) *Arch. Biochem. Biophys.* 377, 178–186.
19. Sander, E. G. (1969) *J. Am. Chem. Soc.* 91, 3629–3634.

20. Schopfer, L. M., Massey, V., and Nishino, T. (1988) *J. Biol. Chem.* 263, 13528–13538.
21. Storer, A. C., and Cornish-Bowden, A. (1976) *Biochem. J.* 159, 1–5.
22. Gibson, Q. H., Swoboda, B. E. P., and Massey, V. (1964) *J. Biol. Chem.* 239, 3927–3934.
23. Jordan, D. B., Bisaha, J. J., and Piccolleli, M. A. (2000) *Arch. Biochem. Biophys.* 378, 84–92.
24. Argyrou, A., and Washabaugh, M. W. (1999) *J. Am. Chem. Soc.* 121, 12054–12062.
25. Krakow, G., and Vennesland, B. (1961) *J. Biol. Chem.* 236, 142–144.
26. Thorpe, C., and Kim, J.-J. P. (1995) *FASEB J.* 9, 718–725.
27. Marcinkeviciene, J., and Blanchard, J. S. (1995) *Biochemistry* 34, 6621–6627.
28. Cenas, N. K., Arscott, D., Williams, C. H., and Blanchard, J. S. (1994) *Biochemistry* 33, 2509–2515.
29. Nakamura, M., and Yamazaki, I. (1972) *Biochim. Biophys. Acta* 267, 249–257.
30. Mesecar, A., D., Stoddard, B. L., and Koshland, D., E., Jr. (1997) *Science* 277, 202–206.
31. Wang, R., and Thorpe, C. (1991) *Biochemistry* 30, 7895–7901.

BI0025666